# Formation of subbands in δ-doped semiconductors

J. Kortus and J. Monecke
*Institute of Theoretical Physics, Freiberg University of Mining and Technology, B.-v.-Cotta-Strasse 4, 09596 Freiberg, Germany*
(Received 27 December 1993)

The formation of the two-dimensional subbands in uncompensated δ-doped semiconductors from single impurity bound states with increasing impurity concentration is calculated using multiple-scattering theory. Previous calculations treated the δ plane as a metallic sheet by solving a one-dimensional Schrödinger equation in a self-consistently screened one-dimensional potential and could not reproduce single impurity bound states in the limit $c \to 0$. In contrast to this approximation multiple-scattering theory can describe well both limits of small and large $c$. The crossover from impurity bands at low concentrations to subbands at large concentrations is discussed and a Mott transition within the δ plane (defined as the vanishing of the gaps in the density of states) is found at $c_{cr} = 9.95 \times 10^{10}\text{cm}^{-2}$ in the case of GaAs:Si.

## I. INTRODUCTION

Recently, there has been a growing interest in the use of atomic plane (δ-) doping techniques due to their potential technological applications for the realization of high-speed electronic[1] and of optoelectronic[2] devices. In the case of GaAs:Si, e.g., shallow Si-impurities substitute Ga-atoms in a (100)-oriented GaAs monolayer. At vanishing impurity concentration individual impurities bind electrons and Coulomb-like bound states are formed. With increasing impurity concentration these bound states are expected to broaden into impurity bands. In the high-density limit the electrons will be confined to the ionized sheet of the impurities and form a two-dimensional electron gas with a two-dimensional subband structure.

Treating the case of an uncompensated δ-doped semiconductor the impurity band formation is entirely due to wave-function overlap and the impurity level broadening by fluctuating classical potentials treated by Shklovskii and Efros[3] has not to be considered.

In the case of a single Si δ-layer in bulk GaAs, theoretical investigation of the electron band structure in the high concentration limit have been performed by several groups in the Hartree,[4] the Thomas-Fermi[5] and in the local density approximations.[6] It has been proved by Ioratti[5] that the semiclassical Thomas-Fermi approximation gives results that are numerically nearly equivalent to those obtained from the much more complicated self-consistent Hartree approximation. Degani[6] has shown, that exchange and correlation effects within the local density approximation have only small influences on the effective potential and the energy band structure in the high-density limit. There are also theoretical investigations of acceptor (Be) δ-doped GaAs (Ref. 7) and of $n$-type uncompensated δ-doped GaAs superlattices.[8] The existence of a two-dimensional electron gas confined in a subband structure has been predicted by these calculations, and has been confirmed by different experimental techniques such as infrared absorption,[9] Raman scattering[10,11] and magnetotransport measurements.[12,13]

All these theories assume, however, that the charge of the ionized impurities is homogeneously smeared out in the δ-doped plane, neglecting the point-charge character of the dopants as well as the spatial potential fluctuations which result from the random distribution of the impurities. We will refer to this jellium approximation as to the metallic sheet approximation. It is expected to be correct in the high-density limit. On the other hand, for vanishing impurity concentration we expect the formation of single impurity bound states. The metallic sheet approximation is not able to reproduce them and becomes wrong at low densities. The aim of the present paper is to present a theory which is correct in both limits of low and high density.

We restrict ourselves to the effective mass approximation, treating the host semiconductor as a homogeneous medium with a dielectric constant $\epsilon$ and the charge carriers as free particles with an effective mass $m^*$. The bare impurity potential is approximated to be a pure Coulomb one.

The screening of the bare Coulomb potentials is a complicated problem, which has been handled in different degrees of sophistication. The best static screening theory available now is to calculate screened potentials self-consistently, as done for disordered solids by Vignale *et al.*[14] combining the coherent potential approximation with the local density approximation. Here we restrict ourselves to the simple Thomas-Fermi screening approximation. It gives the correct high-density limit as well the correct limit at vanishing impurity density. Details of this calculation will be presented in Sec. II of this paper.

The density of states of the impurity bands in the approximation of a nonfluctuating impurity density will show sharp cutoffs and no band tails. Band tails could be obtained either by the optimum fluctuation method[15–17] or by the more simplified method of Serre *et al.*[18] In this contribution, we do not attempt to calculate band tails

 

but restrict ourselves to treat disorder without taking density fluctuations into account.

The standard method to do this is the coherent potential approximation (CPA).[19,20] Until now it cannot be applied to the present case of long range and, hence, overlapping impurity potentials.[21] Already in 1961 Klauder[22] proposed a simplified version of the CPA, the Klauder $V$ approximation, in which so-called multiple occupancy corrections are neglected, and which can be applied to overlapping potentials. This neglection should be tolerable at the usual impurity concentrations. However, as shown by Monecke[23] and by Monecke *et al.*,[24] the self-energy $M$ in the Klauder $V$ approximation reproduces correctly the self-energy $M|_{c=0}$ in the limit of a vanishing impurity concentration $c$, but not its first derivative with respect to the concentration $\frac{dM}{dc}|_{c=0}$ at energies near those of bound states, in which we are just interested. Therefore we will use a linear approximation $M = M|_{c=0} + c\frac{dM}{dc}|_{c=0}$ for the calculation of impurity bands.

In Sec. II we will calculate the screening of bare Coulomb potentials by a two-dimensional electron gas confined by the same and not by external potentials. In Sec. III we will present the treatment of disorder. Results will be presented in Sec. IV and conclusions are given in Sec. V.

## II. SCREENING OF AN IMPURITY BY A TWO-DIMENSIONAL ELECTRON GAS

The screening of an impurity by a two-dimensional electron gas will be calculated in the same approximations (Thomas-Fermi approximation to the kinetic energy of the electrons, linear response of the induced density to the self-consistent potential, neglect of exchange and correlation energy, high density limit) leading to the well-known Thomas-Fermi screened impurity potential

$$v(\mathbf{r}) = -\frac{2}{r}\, e^{-k_{FT}r}, \quad k_{FT}^2 = 4\left(\frac{3n}{\pi}\right)^{1/3}$$

in the three-dimensional case.

Lengths are measured in units of the effective Bohr radius $a_B$ and energies are measured in effective Rydberg ($\hbar = 2m^* = \frac{e^2}{\epsilon} = 1$) in the following. In contrast to the case of quantum wells it is impossible to use the well-known two-dimensional screening result given, e.g., in Refs. 25 and 26, because the electrons are confined by the screened potentials themselves and not by an external potential, the confinement of the electrons and not only the screening vanishes with vanishing electron concentration.

The total Thomas-Fermi energy is given by

$$E = \int d\mathbf{r}\left[\frac{3}{5}\,(3\pi^2)^{2/3}\, n^{5/3}(\mathbf{r}) - 2\int d\mathbf{r}'\frac{\rho(\mathbf{r}')n(\mathbf{r})}{|\,\mathbf{r}-\mathbf{r}'\,|} + \int d\mathbf{r}'\frac{n(\mathbf{r}')n(\mathbf{r})}{|\,\mathbf{r}-\mathbf{r}'\,|}\right], \tag{1}$$

where $\mathrm{n}(\mathbf{r})$ and $\rho(\mathbf{r})$ are the electron and impurity densities, respectively. Minimizing $E$ under the constraint of a constant number of electrons, $\delta\left[\mathrm{E} - \mu\int \mathrm{n}(\mathbf{r})\mathrm{d}\mathbf{r}\right] = 0$, we obtain

$$n(\mathbf{r}) = a\,[\mu - V(\mathbf{r})]^{3/2}, \; a = \frac{1}{3\pi^2}, \tag{2}$$

with $\mu$ being the Fermi energy to be determined later and

$$V(\mathbf{r}) = -2\int d\mathbf{r}'\frac{\rho(\mathbf{r}') - n(\mathbf{r}')}{|\,\mathbf{r}-\mathbf{r}'\,|}. \tag{3}$$

Due to the charge neutrality we have $\int d\mathbf{r}n(\mathbf{r}) = \int d\mathbf{r}\rho(\mathbf{r})$.

For the subsequent application of single site multiple-scattering theory in Sec. III we have to require that the Fourier transformed screened potential can be written in the form $V(\mathbf{k}) = \Omega v(\mathbf{k})\rho(\mathbf{k})$ with the structure factor $\rho(\mathbf{k})$ of the impurity distribution. This corresponds to the neglection of, e.g., covalent bonding leading to "forbidden" reflexes. The common charge cloud of two impurities then is simply the superpositon of their individual charge clouds independent of the distance. This is ensured linearizing (2) with the result

$$n(\mathbf{r}) = a\mu^{3/2} - \frac{3}{2}a\mu^{1/2}V(\mathbf{r}). \tag{4}$$

As in the three-dimensional case this linearization of the response can be justified only a posteriori. $V(\mathbf{r})$ in (2) is not small compared to $\mu$ the regions of small $n(\mathbf{r})$. But in these regions the Thomas-Fermi theory itself becomes wrong due to its statistical character. Its failure results in a power law $\sim \frac{1}{r^6}$ decrease of the self-consistent $n(\mathbf{r})$ away from a single impurity, respectively, $n(z) \sim \frac{1}{z^6}$ in the two-dimensional case.[5] The linear response theory results in both cases in the expected exponential decrease of $n(\mathbf{r})$ (see below).

Hence, the linearized theory describes better the screening charge cloud around one given impurity than the full one, neglecting charge redistributions between impurities, however.

The compensation of the errors of the Thomas-Fermi theory itself with that of its linearization never has been fully understood, the use of the linearized Thomas-Fermi theory can be justified by its evident successes in all considered applications only.

From (3) we obtain

$$\Delta V(\mathbf{r}) = -8\pi[\rho(\mathbf{r}) - n(\mathbf{r})]. \tag{5}$$

The Fourier transformation

$$V(\mathbf{q}) = \frac{1}{\Omega}\int d\mathbf{r}e^{i\mathbf{q}\cdot\mathbf{r}}V(\mathbf{r}),$$

$$V(\mathbf{r}) = \frac{\Omega}{(2\pi)^3}\int d\mathbf{q}e^{-i\mathbf{q}\cdot\mathbf{r}}V(\mathbf{q})$$

of (5) then gives together with that of (4) the self-consistent potential

$$V(\mathbf{q}) = -\frac{8\pi}{q^2 + k_{FT}^2}\rho(\mathbf{q}) + \frac{2}{3}\mu\delta^3(\mathbf{q}) \tag{6}$$

with

$$n(\mathbf{q}) = \frac{k_{FT}^2}{q^2 + k_{FT}^2}\rho(\mathbf{q}) \tag{7}$$

and

$$k_{FT}^2 = 12\pi a\mu^{\frac{1}{2}}. \tag{8}$$

$\delta^3(\mathbf{r})$ and $\delta^3(\mathbf{q})$ are normalized here in such a way that

$$\frac{\Omega}{(2\pi)^3}\int d\mathbf{q}\delta^3(\mathbf{q}) = 1 \quad \text{and} \quad \frac{1}{\Omega}\int d\mathbf{r}\delta^3(\mathbf{r}) = 1\ .$$

In the high-density limit we can approximate the $\delta$-doped layer as a metallic sheet replacing $\rho(\mathbf{r})$ by its averaged value $\langle\rho(\mathbf{r})\rangle$ over all possible impurity positions within the $z = 0$ plane

$$\begin{aligned}\langle\rho(\mathbf{r})\rangle &= \frac{c}{L}\delta(z),\\ \langle\rho(\mathbf{q})\rangle &= \frac{c}{L}\delta(q_x)\delta(q_y),\end{aligned} \tag{9}$$

where $c$ is the two-dimensional impurity concentration given by

$$\int \rho(\mathbf{r})d\mathbf{r} = cF = c\int dxdy. \tag{10}$$

From (7) we obtain

$$n(\mathbf{q}) = \frac{k_{FT}^2}{q^2 + k_{FT}^2}\frac{c}{L}\delta(q_x)\delta(q_y), \tag{11}$$

or

$$n(\mathbf{r}) = \frac{\Omega}{(2\pi)^3}\int d\mathbf{q}e^{-i\mathbf{q}\cdot\mathbf{r}}n(\mathbf{q}) = n(z) = \frac{ck_{FT}}{2}e^{-k_{FT}|z|}, \tag{12}$$

and from (4)

$$V(z) = \frac{2}{3}\mu - 8\pi\frac{1}{k_{FT}^2}n(z). \tag{13}$$

The Fermi energy $\mu$, and therefore $k_{FT} = \sqrt{12\pi a\mu^{1/2}}$, remains to be determined using the high-density results (12) and (13).

For neutral systems $\mu$ cannot be obtained from the constraint $N = \int n(\mathbf{r})d\mathbf{r}$, which is satisfied automatically in the linearized Thomas-Fermi theory [$n(\mathbf{q} = 0) = \rho(\mathbf{q} = 0)$, see (7)].

In the corresponding three-dimensional linear response case $\mu$ can be obtained from

$$\mu = \frac{\delta E}{\delta N} = \frac{\delta N\varepsilon}{\delta N} = \varepsilon + n\frac{\partial\varepsilon}{\partial n}, \tag{14}$$

with $\varepsilon$ being the energy per electron and $n$ being the three-dimensional concentration, approximating $E$ in the high-density limit by its kinetic energy contribution $E_{\text{kin}} = \int d\mathbf{r}\frac{3}{5}(3\pi^2)^{2/3}n^{5/3}$. In the two-dimensional case all contributions to $E$ have the same $c$ dependence ($\sim c^{9/5}$) as $E_{\text{kin}}$, however, and we have to use the full expression (1).

In the case of the full (nonlinearized) Thomas-Fermi theory $\mu$ can be obtained by the following equivalent methods: First from (14) with $E = E_{\text{kin}} + E_{\text{pot}}$. From (4) we obtain with the choice of the energy zero so that $V(z = 0) = 0$,

$$n(z = 0, \mu) = a\mu^{3/2} \tag{15}$$

as a second self-consistent equation for the determination of $\mu$.

The integration of (2) results in

$$\mu N = \int (3\pi^2)^{2/3}n^{5/3}(\mathbf{r}, \mu)d\mathbf{r} + \int V(\mathbf{r}, \mu)n(\mathbf{r}, \mu)d\mathbf{r} \tag{16}$$

as another equation for $\mu$.

$E_{\text{kin}}$ and $E_{\text{pot}} = \int V'(\mathbf{r})n(\mathbf{r})d\mathbf{r}$ with $V' = V - \mu$ are related by the virial theorem in the Thomas-Fermi approximation

$$\frac{5}{3}E_{\text{kin}} = -E_{\text{pot}}, \tag{17}$$

which again leads to a self-consistent $\mu$ determination.

Within the full nonlinearized Thomas-Fermi theory[5] the results for $\mu$ naturally coincide. This, however, is not the case in the linear response theory. Here, the potential $V(\mathbf{r})$ obtained from (13) does not exactly minimize $E$. The error in $V(\mathbf{r})$, however, is differently weighted by the methods mentioned, leading together with (12) and (13) to different results for $k_{FT}$ : $k_{FT} = 1.5788 \times c^{1/5}$, $k_{FT} = 1.9816\times c^{1/5}$, $k_{FT} = 1.9472\times c^{1/5}$ and $k_{FT} = 1.3927\times c^{1/5}$ for the above given four possiblities, respectively. Within the Thomas-Fermi approximation the kinetic energy is given only in a relatively rough approximation, leading to the unusual virial theorem $\frac{5}{3}E_{\text{kin}} = -E_{\text{pot}}$. We, therefore, tried to obtain additionally a more reliable result by the following method.

Multiplying the self-consistent (not the bare) potential $V'(\mathbf{r})$ by an arbitrary coupling constant $\lambda$, the Hellmann-Feynman theorem $\frac{\partial E}{\partial\lambda} = (\psi, \frac{\partial H}{\partial\lambda}\psi)$ leads to

$$E = E_{\text{kin}}(\lambda = 0) + \int_0^1 d\lambda\frac{1}{\lambda}E_{\text{pot}}(\lambda). \tag{18}$$

In our case, we have $E_{\text{kin}}(\lambda = 0) = 0$ due to $\frac{1}{\Omega}\int n(\mathbf{r})d\mathbf{r} = 0$ and

$$E_{\text{pot}}(\lambda) = \int n(\mathbf{r}, \lambda)V'(\mathbf{r}, \lambda)d\mathbf{r} = \lambda^2\int n(\mathbf{r})V'(\mathbf{r})d\mathbf{r}$$

due to $n \sim V'$. From (18) we obtain then

$$2E_{\text{kin}} = -E_{\text{pot}}. \tag{19}$$

This equation results together with (12) and (13) in

$$k_{FT} = 1.2484c^{1/5} \tag{20}$$

as a further possible function $k_{FT}(c)$.

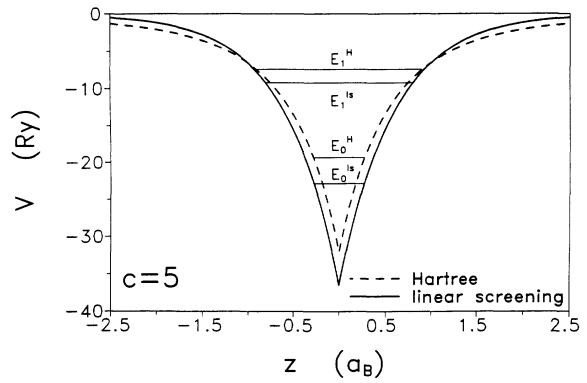


FIG. 1. The self-consistent Hartree potential and the potential of the linearized Thomas-Fermi theory ($k_{FT} = 1.2484c^{1/5}$) for $c = 5\ a_B^{-2}$ and the corresponding two lowest subband bottoms.

The uncertainty in the determination of $k_{FT}$ is inherent to a linear response theory and cannot be circumvented by any mean. It does not occur in the three-dimensional linear response case because there in the high density limit $E$ can be approximated by $E_{\rm kin}$, $V(\mathbf{r})$ not being involved at all.

Because the screening within any Thomas-Fermi approximation always is too large, we decided to use the smallest $k_{FT}$ given by (20) in the following calculations.

In Fig. 1 we show the potential $V(z)$ obtained in this way in comparision with the self-consistent Hartree potential,[6] which is well approximated by that of the full Thomas-Fermi one,[5] together with the two lowest eigenvalues (subband bottoms) for $c = 5$. We did not try to choose $k_{FT}$ in such a way that these eigenvalues coincide, the difference not being of essential importance for the subsequent calculations.

From (6) and $V(\mathbf{q}) = \Omega v(\mathbf{q})\rho(\mathbf{q}) + \frac{2}{3}\mu\delta^3(\mathbf{q})$, we get

$$v(\mathbf{r}) = \frac{\Omega}{(2\pi)^3}\int d\mathbf{q} e^{-i\mathbf{q}\cdot\mathbf{r}} v(\mathbf{q}) = -\frac{2}{r}e^{-k_{FT}r} \qquad (21)$$

for one single, screened by a two-dimensional electron gas, impurity potential at the origin. This expression was derived from the high-density (metallic) limit but reproduces the $c = 0$ limit as well [Eq. (20)]. So we can expect that a multiple-scattering theory using this potential results in two-dimensional subbands for large $c$ and in single impurity bound states for $c \to 0$.

## III. THE SMALL CONCENTRATION APPROXIMATION FOR THE SELF-ENERGY

The equation of motion for the one-particle Green's function in the effective mass approximation is

$$G(\mathbf{k},\mathbf{k}') = G^0(\mathbf{k})\delta^3(\mathbf{k}-\mathbf{k}') + G^0(\mathbf{k})\frac{\Omega}{(2\pi)^3}\int d\mathbf{q} V(\mathbf{k}-\mathbf{q})G(\mathbf{q},\mathbf{k}') , \qquad (22)$$

with

$$G^0(\mathbf{k}) = \left[E - \mathbf{k}^2\right]^{-1} \qquad (23)$$

and $V(\mathbf{k}-\mathbf{q})$ being given by (6).

The averaged over all possible impurity configurations in the $z = 0$ plane Green's function $\bar{G}(\mathbf{k},\mathbf{k}') = \langle G(\mathbf{k},\mathbf{k}')\rangle_{\rm av}$ obeys an equation similar to (22).

$$\bar{G}(\mathbf{k},\mathbf{k}') = G^0(\mathbf{k})\delta^3(\mathbf{k}-\mathbf{k}') + G^0(\mathbf{k})\frac{\Omega}{(2\pi)^3}\int d\mathbf{q} M(\mathbf{k},\mathbf{q};E)\bar{G}(\mathbf{q},\mathbf{k}'), \qquad (24)$$

which defines the self-energy $M(\mathbf{k},\mathbf{q};E)$ as a nonlocal energy-dependent average potential.

Equation (22) may be solved formally by iteration. For the calculation of $\bar{G}(\mathbf{k},\mathbf{k}')$ the averages

$$M_n(\mathbf{p}_1\cdots\mathbf{p}_n) = \langle\rho(\mathbf{p}_1)\rho(\mathbf{p}_2)\cdots\rho(\mathbf{p}_n)\rangle_{\rm av} \qquad (25)$$

have to be calculated, then.

The same approximation as in Ref. 24, which is correct linear in $c$, and corresponds to the average $t$-matrix approximation, results for the two-dimensional case in

$$M(\mathbf{k},\mathbf{k}';E) = \frac{c}{L}\delta^2(\mathbf{k}_2-\mathbf{k}_2')t(\mathbf{k},\mathbf{k}';E), \qquad (26)$$

with $\mathbf{k}_2 = (k_x, k_y)$, where

$$t(\mathbf{k},\mathbf{k}';E) = v(\mathbf{k}-\mathbf{k}') + \frac{1}{(2\pi)^3}\int d\mathbf{q} v(\mathbf{k}-\mathbf{q})G^0(\mathbf{q})t(\mathbf{q},\mathbf{k}';E) \qquad (27)$$

is the $t$ matrix and $v(\mathbf{k})$ is the potential of one impurity, both multiplied by the total volume $\Omega$.

As in the three-dimensional case the self-energy linear in $c$ is equal to the $t$ matrix of one impurity, multiplied by the concentration and a $\delta$ function ensuring momentum conservation, here in the x-y plane only. The corresponding result is true in the one-dimensional case, too.

Substituting (26) into (24) one obtains for $\bar{G}(\mathbf{k},\mathbf{k}')$ the equation

$$\bar{G}(\mathbf{k},\mathbf{k}') = G^0(\mathbf{k})\delta^3(\mathbf{k}-\mathbf{k}') + G^0(\mathbf{k})\frac{c}{2\pi}\int dq_z t(\mathbf{k},\mathbf{q};E)G(\mathbf{q},\mathbf{k}';E) , \qquad (28)$$

where $\mathbf{q} = (k_x, k_y, q_z)$.

The solution of (28) is given by

$$\bar{G}(\mathbf{k},\mathbf{k}') = \delta^2(\mathbf{k}_2-\mathbf{k}_2')\bar{G}(k_z,k_z';\mathbf{k}_2) . \qquad (29)$$

$\bar{G}(k_z,k_z';\mathbf{k}_2)$ obeys the integral equation

$$\bar{G}(k_z,k_z',\mathbf{k}_2) = G^0(k_z,\mathbf{k}_2)\delta(k_z-k_z') + G^0(k_z,\mathbf{k}_2)\frac{c}{2\pi} \times \int dq_z t(k_z,q_z,\mathbf{k}_2;E)\bar{G}(q_z,k_z',\mathbf{k}_2) , \qquad (30)$$

with $\mathbf{k}_2$ as a parameter.

Hence, due to the restricted to a plane momentum conservation, we cannot obtain the average Green's function in the form

$$\bar{G}(\mathbf{k}) = [E - \mathbf{k}^2 - M(\mathbf{k}, E)]^{-1} \tag{31}$$

as in the three-dimensional case, but have to solve the one-dimensional integral equation (30) after the solution of the three-dimensional integral Eq. (25).

## IV. RESULTS

The numerical solution of the three-dimensional integral Eq. (27) as given in subsection (C) is a very time consuming step and before performing it we try to avoid this step by two simple approximations given in the subsections (A) and (B).

### A. Simpliest approximation, $t(\mathbf{k}, \mathbf{k}'; E) = v(\mathbf{k} - \mathbf{k}')$

We approximate $t(\mathbf{k}, \mathbf{k}'; E)$ by its leading term $v(\mathbf{k} - \mathbf{k}')$ and obtain the following self-energy

$$M(\mathbf{k}, \mathbf{k}'; E) = \frac{c}{L}\delta^2(\mathbf{k_2} - \mathbf{k_2'})v(k_z - k_z') \ . \tag{32}$$

The solution of (24) then just corresponds to the solution of the one-dimensional Schrödinger equation

$$\left(-\frac{d^2}{dz^2} + V(z)\right)\psi(z) = E\psi(z) \ , \tag{33}$$

with

$$\begin{aligned} V(z) &= \frac{\Omega}{(2\pi)^3}\int d\mathbf{k} e^{-i\mathbf{k}\cdot\mathbf{r}} M(\mathbf{k}, \mathbf{k}'; E) \\ &= -\frac{4\pi c}{k_{FT}} e^{-k_{FT}|z|} \end{aligned} \tag{34}$$

being given by (8), (12), and (13). The energy zero is choosen so that $V(z = \infty) = 0$. Hence, the replacement of $t(\mathbf{k}, \mathbf{k}'; E)$ by $v(\mathbf{k} - \mathbf{k}')$ just reproduces the metallic sheet result (high-density limit) usually considered.

The solutions of (33) have the well-known form of parabolic subbands

$$E = E_i + k_x^2 + k_y^2 \ , \tag{35}$$

with the $E_i$ shown in Fig. 2. These $E_i$ obtained in the linearized Thomas-Fermi approximation only slightly deviate from the results of the nonlinear Thomas-Fermi and of Hartree calculations.[5,6]

For $c \to 0$ the effective potential $V(z)$ [Eq. (34)] vanishes and the metallic sheet approximation results in the conduction band only, being not able to reproduce the bound states of single impurities. The corrections to this approximation by the separable potential approach (B) or the full expression (C) of the $t$ matrix is not small in this limit, because the $t$ matrix has poles at the energies of the bound states of the one impurity problem, in which energy region we are just interested.

### B. Separable potential approach

The numerical solution of the integral Eq. (26) can be avoided using an artifical techniques first applied to our knowledge by Haug and Tran.[27] We replace the potential $v(\mathbf{k} - \mathbf{k}')$ by the so-called separable potential in the same way as described in detail by, e.g., Gold *et al.*[28] and Monecke *et al.*[24] This approach is applied to the calculation of the self-energy $M$ only, not to the integral equation for the averaged Green's function. (27) then reduces to an algebraic equation, and we obtain for the self-energy the approximation

$$M(\mathbf{k}, \mathbf{k}'; E) = \frac{c}{L}\delta(\mathbf{k}_2 - \mathbf{k}'_2)\frac{v(k_z - k_z')}{1 - \frac{1}{k_{FT} + \sqrt{-E}}} \ . \tag{36}$$

This self-energy has a pole, which reproduces for $c = 0$ the lowest bound state of one single impurity at $E = -1$ Ry. Hence, we obtain even for $c \to 0$ a finite self-energy

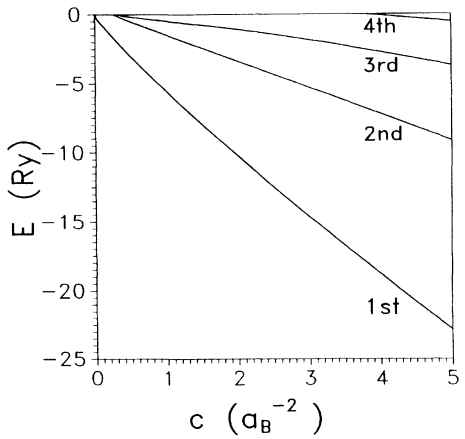


FIG. 2. The lowest four subband bottom energies $E_i$ as a function of the concentration $c$ in the approximation $t(\mathbf{k}, \mathbf{k}'; E) = v(\mathbf{k} - \mathbf{k}')$.

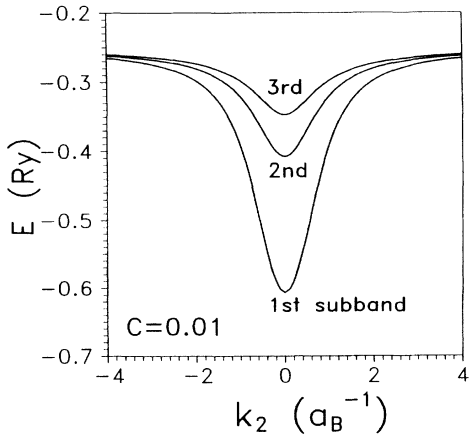


FIG. 3. Dispersion relation $E(k)$ with $k = \sqrt{k_x^2 + k_y^2}$ for the three lowest subbands at $c = 0.01\ a_B^{-2}$ ($1.03 \times 10^{10}$ cm$^{-2}$ in the case of GaAs:Si) within the separable potential approximation.

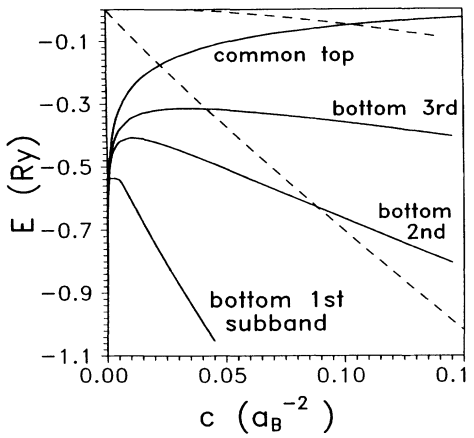


FIG. 4. The three lowest subband bottom energies $E_i$ (solid lines) within the separable potential approximation in comparision to those of the simpliest approximation $t(\mathbf{k},\mathbf{k}';E) = v(\mathbf{k}-\mathbf{k}')$ (dashed lines) as a function of the concentration. The common band top ($k = \infty$) is indicated by "top."

near the bound state of one impurity. The separable potential approach can principally result in one ($s$-like) bound state only. We expect the solution of (24) with (36) to result below the conduction band for small $c$ in one impurity band obtained from this bound state and in the usual subbands for large $c$, where (36) becomes identical with (32).

In the approximations (32) and (36) the different roles of the $\mathbf{k}_2$ vector should be considered carefully. $\mathbf{k}_2 = (k_x, k_y)$ occurs in (24) with (36) only through $G^0(\mathbf{k})$, it means as an additive term $k_2^2$ to $E$. However, this will not result in parabolic bands as in the simpliest approximation $t(\mathbf{k},\mathbf{k}';E) = v(\mathbf{k}-\mathbf{k}')$ due to the additional $E$ dependence of the self-energy $M$ without an additive $k_2^2$. In Fig. 3 we present the dispersion relation for the three lowest bands as a function of $k = |\mathbf{k}_2|$. For $k \to \infty$ all bands result in the same top given by the bound state energy of one screened Coulomb potential (see C). For $c \to 0$ all these bands degenerate into one straight line at the energy of the bound state of one unscreened impurity.

Figure 4 shows the impurity band bottoms and the common band top as a function of the concentration in comparision to the results of the first approximation.

Figure 5 shows the effective mass $m^{**}$ at the bottom of the impurity bands as a function of $c$. In contrast to the metallic sheet approximation it deviates strongly from the conduction band mass $m^*$ and even diverges for $c \to 0$.

The density of states of the lowest impurity band is plotted for $c = 0.01$ in Fig. 6. It is small near the bottom of the band and shows here a behaviour similar to the stepwise one of the metallic sheet approximation.[1] The deviations from the latter are due to the deviations of the dispersion curve from a parabolic approximation. It becomes infinite at the band top due to the flatness of the $E(k)$ curve for large $k$ (see Fig. 3). This divergency is an artefact of the effective-mass approximation caused by the lack of a Brillouin zone boundary at finite $\mathbf{k}$ vectors.

For $c \to \infty$, the screening length $k_{FT}$ [see Eq. (22)] goes to infinity, that means that

$$\lim_{c\to\infty}\left(1 - \frac{1}{k_{FT} + \sqrt{-E}}\right) = 1 \qquad (37)$$

at any energy.

The pole in the self-energy $M$ becomes unimportant and Eq. (36) reduces to (32). Hence we obtain the same results as in the first approximation (e.g., the same subband energies $E_i$, parabolic bands and effective masses $m^{**} \to m^*$).

The separable potential approach shows, however, one serious physical error: $M$ given by (36) besides possessing only one pole at $E = -1$ Ry shows a wrong $\mathbf{k}$ dependence, which results in wrong symmetry properties. As a consequence all subbands (of alternating even and odd parity for $c \to \infty$) degenerate to the same $s$-like bound state

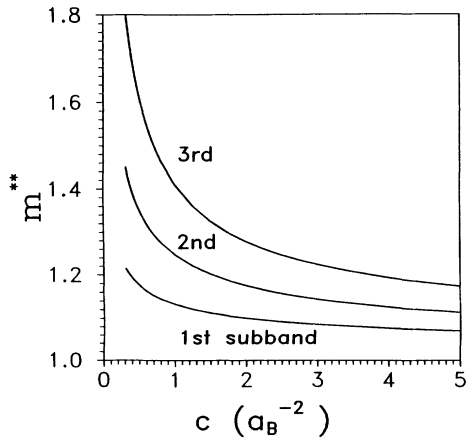


FIG. 5. Concentration dependence of the effective masses $m^{**}$ (in units of $m^*$) close to the bottoms of the three lowest subbands within the separable potential approximation.

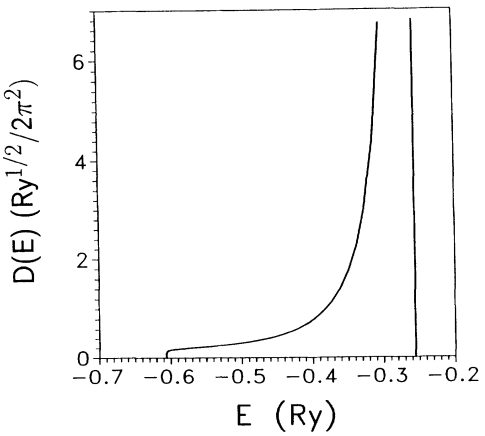


FIG. 6. Density of states inside the first impurity subband obtained from the dispersion $E(k)$ in Fig. 3 for $c = 0.01\ a_B^{-2}$ ($1.03 \times 10^{10}$ cm$^{-2}$ in the case of GaAs:Si) within the separable potential approximation.

with vanishing $c$, which physically is impossible. From a superposition of $s$-like states no odd subband can be obtained in a reliable approximation. We expect in contrast to this the lowest subband to shrink with $c \to 0$ to the $s$-like bound state at $E = -1$ Ry, the next subband of even parity to shrink to the $p_z$ state at $E = -\frac{1}{4}$ Ry and so on, a behavior which principially cannot be obtained with separable potentials.

### C. Exact numerical solution of $t(\mathbf{k}, \mathbf{k}'; E)$

In order to obtain reliable results for the self-energy Eq. (27) was solved numerically, discretizing it to a set of linear equations which was solved exactly. The resulting $t$ matrix was used then to determine the poles of (30). The results for $|\ \mathbf{k}_2\ | = 0$ and $|\ \mathbf{k}_2\ | = \infty$ are shown in Fig. 7.

For small $c$ the lowest band bottom starts correctly from $E = -1$ Ry. It first rises rapidly and then moves downward parallel to the lowest subband bottom obtained from the metallic sheet approximation. The corresponding $1s$ band top starts at $-1$ Ry, too, and rises continuously. Therefore, the dispersion relation for large $c$ becomes parabolic near the band bottom (see below). The next subband bottom (of odd parity for large $c$) starts at $E = -\frac{1}{4}$ Ry for $c = 0$. Obviously it is derived from the $2p_z$ state. Its top rises rapidly, so that it cannot be drawn using the scale of Fig. 7. The third subband bottom (of even parity for large $c$) could be distinguished numerically from the second one only down to about $c = 0.02 \cdot a_B^{-2}$. We believe it to start from the $2s$, $2p_x$, and $2p_y$ states at $c = 0$.

For $|\ \mathbf{k}_2\ | \to \infty$ we have $G^0(\mathbf{k}) \to 0$ and (30) has a solution with $\bar{G} \neq 0$ only at the poles of the one-impurity $t$ matrix. The impurity band top energies therefore coincide exactly with the bound state energies of single impurities. The same is true in the case of the separable potential approximation, the common band top in this case being given by the pole at $E = -(1 - k_{FT})^2$ of (36). Our numerical solutions for $|\ \mathbf{k}_2\ | \to \infty$ agree fairly well with the results of Yukawa bound state calculations (see, e.g., Rogers *et al.*[29]), indeed. This is valid in all dimensions and is exact within the average $t$-matrix approximation, i.e., linear in $c$.

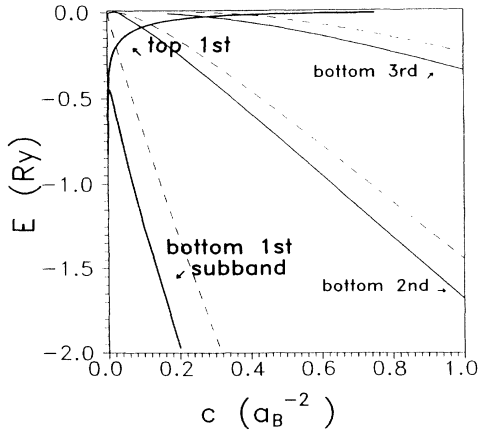


FIG. 7. Concentration dependence of the bottoms of the three lowest subbands and the $1s$-band top (solid lines) in comparision to those of the first approximation $t(\mathbf{k}, \mathbf{k}'; E) = v(\mathbf{k} - \mathbf{k}')$ (dashed lines).

The fact, that the $1s$-band top merges the conduction band just at the concentration at which one single screened potential has no bound state ($c = 0.79 a_B^{-2}$ corresponding to $c = 8.1 \times 10^{11}\text{cm}^{-2}$ for GaAs:Si in our approximations) corresponds to the early suggestion of Mott and Davies[30] for the critical concentration of insulator-to-metal transitions.

But well below this concentration the top of the $1s$-band merges with the bottom of the $2p_z$ band (here at $c_{cr} = 0.097 a_B^{-2}$ corresponding to $c_{cr} = 9.95 \times 10^{10}\text{cm}^{-2}$ in the case of GaAs:Si). Due to the steep rise of all other band tops with $c$ for concentrations above $c_{cr}$ no other gaps between higher impurity bands are expected. Therefore, $c_{cr}$ is the critical concentration of the insulator to metal transition, defined as the concentration at which all gaps close (calculating an averaged one particle Green's function only no information about the expected Anderson localization[31] of the states can be obtained, of course).

In the high-density limit ($c \to \infty$, $k_{FT} \to \infty$) we are far away from the energies of one impurity bound states and, hence, we can treat (27) as an absolutly convergent Neumann series

$$t(\mathbf{k}, \mathbf{k}'; E) = v(\mathbf{k} - \mathbf{k}') + \frac{1}{(2\pi)^3} \int d\mathbf{q} v(\mathbf{k} - \mathbf{q}) G^0(\mathbf{q}) v(\mathbf{q} - \mathbf{k}') + \dots \,. \tag{38}$$

With the help of the mean value theorem of the integral calculus we obtain

$$t(\mathbf{k}, \mathbf{k}'; E) = v(\mathbf{k} - \mathbf{k}') + v(\mathbf{k} - \zeta) G^0(\zeta) v(\zeta - k') + \dots \,. \tag{39}$$

For large $c$ (respectively, $k_{FT}$) the formfactor $v$ is proportional to $0(k_{FT}^{-2})$ and neglecting higher orders we get

$$t(\mathbf{k}, \mathbf{k}'; E) \approx v(\mathbf{k} - \mathbf{k}') \,, \tag{40}$$

which results in the same self-energy as (32).

Hence, for large $c$ the impurity bands become identical with the subbands obtained from the metallic sheet approximation.

## V. CONCLUSIONS

Avoiding the metallic sheet approximation we described a $\delta$ layer as a system of randomly distributed impurities in a plane and applied multiple-scattering theory to obtain the averaged one particle Green's function and, hence, the mean eigenvalue spectrum.

It was demonstrated that for very small concentrations

the eigenvalues coincide with the bound state eigenvalues of single unscreened impurities. With increasing concentration in the uncompensated case impurity bands are formed by wave-function overlap. These bands have effective masses deviating from the host semiconductor conduction band mass and densities of states deviating from the stepwise behavior of the metallic sheet approximation. For large $c$ the latter approximation becomes exact and the impurity bands can be described in terms of the well-known two-dimensional subbands.

This qualitative behaviour does not depend on the special approximations choosen, the linear response screening theory for $k_{FT}$ obtained from the high-density limit and the average $t$-matrix approximation. Both approximations influence results only quantitatively.

Defining the critical concentration of the insulator-to-metal transition as the concentration at which all gaps between the impurity bands close, we obtain $c_{cr} = 9.95 \times 10^{10}\text{cm}^{-2}$ in the case of GaAs:Si. Below this concentration the subband concept clearly has no meaning.

Using a single-site multiple-scattering theory we could not obtain extended band tails caused by impurity density fluctuations. Likewise, no information about the extended, respectively, localized nature of the impurity band states could be obtained. These points need further investigations.

## ACKNOWLEDGMENTS

One of the authors (J.K.) gratefully acknowledge the Land Sachsen for financial support.

[1] E. O. Göbel and K. Ploog, Prog. Quantum Electron. **14**, 289 (1990), and references therein.
[2] G. H. Döhler, Phys. Status Solidi **52**, 79 (1972).
[3] B. I. Shklovskii and A. L. Efros, in *Electronic Properties of Doped Semiconductors*, edited by M. Cardona, P. Fulde, and M.-J. Queisser, Springer Series in Solid-State Sciences Vol. 45 (Springer, Berlin, 1984).
[4] A. Zrenner, F. Koch, and K. Ploog, Surf. Sci. **196**, 671 (1988).
[5] L. Ioratti, Phys. Rev. B **41**, 8340 (1990).
[6] M. H. Degani, Phys. Rev. B **44**, 5580 (1991).
[7] F. A. Roboredo and C. R. Proetto, Phys. Rev. B **47**, 4655 (1993).
[8] F. A. Roboredo and C. R. Proetto, Solid State Commun. **81**, 163 (1992).
[9] N. Schwarz, F. Müller, G. Tempel, F. Koch, and G. Weiman, Semicond. Sci. Technol. **4**, 671 (1988).
[10] G. Abstreiter, R. Merlin, and A. Pinczuck, IEEE J. Quantum Electron. **QE-22**, 1771 (1986).
[11] J. Wagner, A. Fisher, and K. Ploog, Phys. Rev. B **42**, 7280 (1990).
[12] F. Koch and A. Zrenner, Mater. Sci. Eng. B **1**, 221 (1989).
[13] A. Zrenner, F. Koch, R. L. Williams, R. A. Stradling, K. Ploog, and G. Weimann, Semicond. Sci. Technol. **3**, 1203 (1988).
[14] G. Vignale, H. Weiler, W. Kanke, and A. A. Maradudin, Z. Phys. B **69**, 209 (1987).
[15] B. I. Halperin and M. Lax, Phys. Rev. **148**, 722 (1966); **153**, 802 (1967).
[16] J. Zittarz and J. S. Langer, Phys. Rev. **148**, 722 (1966).
[17] I. M. Lifshitz, Zh. Eksp. Theor. Fiz. **53**, 743 (1967) [Sov. Phys. JETP 26, 462 (1968)].
[18] J. Serre, A. Ghazali, and P. Levoux Hugon, Phys. Rev. B **23**, 1971 (1981).
[19] P. Soven, Phys. Rev. **156**, 809 (1967).
[20] B. Velicky, S. Kirkpatrick, and H. Ehrenreich, Phys. Rev. **175**, 747 (1968).
[21] J. Serre and A. Ghazali, Phys. Rev. B **28**, 4704 (1983).
[22] J. R. Klauder, Ann. Phys. (N.Y.) **14**, 43 (1961).
[23] J. Monecke, Phys. Status Solidi B **152**, 123 (1989).
[24] J. Monecke, J. Kortus, and W. Cordts, Phys. Rev. B **47**, 9377 (1993).
[25] T. Ando, A. Fowler, and F. Stern, Rev. Mod. Phys. **54**, 437 (1982).
[26] G. Bastard, *Wave Mechanics Applied to Semiconductor Heterostructures* (Editions de Physique, Les Ulis, 1988).
[27] H. Haug and D. B. Tran Thoai, Phys. Status Solidi B **98**, 581 (1980).
[28] A. Gold, J. Serre, and A. Ghazali, Phys. Rev. B **37**, 4589 (1988).
[29] F. J. Rogers, H. C. Graboske, Jr., and D. J. Harwood, Phys. Rev. A **6**, 1577 (1970).
[30] N. F. Mott and J. H. Davies, Philos. Mag. B **42**, 845 (1980).
[31] P. W. Anderson, Phys. Rev. **109**, 1492 (1958).